Published in final edited form as:

Prostaglandins Other Lipid Mediat. 2021 February ; 152: 106485. doi:10.1016/j.prostaglandins.2020.106485.

20-HETE Interferes with Insulin Signaling and Contributes to Obesity-Driven Insulin Resistance

Ankit Gilani[1], **Kevin Agostinucci**[1], **Sakib Hossain**[1], **Jonathan V. Pascale**[1], **Victor Garcia**[1], **Adeniyi Michael Adebesin**[2], **John R. Falck**[2], **Michal Laniado Schwartzman**[1]

[1]Department of Pharmacology, New York Medical College School of Medicine, Valhalla, NY

[2]Department of Biochemistry, University of Texas Southwestern Medical Center, TX

Abstract

20-HETE, a metabolite of arachidonic acid produced by Cytochrome P450 (CYP) 4A/4F, has been implicated in the development of obesity-associated complications such as diabetes and insulin resistance. In this study, we examined whether the acute elevation of 20-HETE levels contributes to the development of diet-driven hyperglycemia and insulin resistance. We employed a conditional transgenic mouse model to overexpress Cyp4a12 (Cyp4a12tg), a murine 20-HETE synthase, together with high fat diet (HFD) feeding. Mice in which Cyp4a12 was induced by doxycycline (DOX) at the onset of HFD feeding gained weight at a greater rate and extent than corresponding DOX-untreated Cyp4a12 mice. Cyp4a12tg mice fed HFD+DOX displayed hyperglycemia and impaired glucose metabolism while corresponding HFD-fed Cyp4a12tg mice (no DOX) did not. Importantly, administration of a 20-HETE antagonist, 20-SOLA, to Cyp4a12tg mice fed HFD+DOX significantly attenuated weight gain and prevented the development of hyperglycemia and impaired glucose metabolism. Levels of insulin receptor (IR) phosphorylation at Tyrosine 972 and insulin receptor substrate-1 (IRS1) phosphorylation at serine 307 were markedly decreased and increased, respectively, in liver, skeletal muscle and adipose tissues from Cyp4a12tg mice fed HFD+DOX; 20-SOLA prevented the IR and IRS1 inactivation, suggesting that 20-HETE interferes with insulin signaling. Additional studies in 3T3-1 differentiated adipocytes confirmed that 20-HETE impairs insulin signaling and that its effect may require activation of its receptor GPR75. Taken together, these results provide strong evidence that 20-HETE interferes with insulin function and contributed to diet-driven insulin resistance.

Keywords

High-Fat Diet; Hyperglycemia; Insulin Resistance; 20-HETE; GPR75

Corresponding Author: Dr. Michal Laniado Schwartzman, Department of Pharmacology, New York Medical College School of Medicine, Valhalla, NY 10595, Michal_schwartzman@nymc.edu.

Declaration of interest

All authors declare that there is no conflict of interest that could be perceived as prejudicing the impartiality of the research reported.

INTRODUCTION

20-Hydroxyeicosatetraenoic acid (20-HETE) is the omega-hydroxylated metabolite of arachidonic acid produced by the Cytochrome P450 (CYP) 4A and 4F family of enzymes. It is a bioactive lipid mediator that promotes vascular smooth muscle contraction, endothelial dysfunction, inflammation and cell proliferation [1]. A recent study from our laboratory identified the orphan G-protein coupled receptor 75 (GPR75) as the 20-HETE receptor through which it signals to affect vascular function [2].

Several studies suggested a role for 20-HETE in the development and progression of obesity, insulin resistance and metabolic syndrome. Clinical studies demonstrated that the urinary and plasma levels of 20-HETE correlate with body to mass index (BMI) and are elevated in obese, diabetic and metabolic syndrome individuals [3–6]. A genetic variant in the *CYP4F2* gene, the main gene implicated in 20-HETE synthesis in humans, was reported as a major risk factor for diabetes post kidney transplant [7]. Studies in animal models have also shown correlations between 20-HETE levels, weight gain and metabolic syndrome [8–11] and that it contributes to hyperglycemia [12] and to the pathogenesis of diabetes including diabetic retinopathy and nephropathy [13–16]. In vitro, 20-HETE stimulates adipogenesis [17], and impedes the cellular actions of insulin [18, 19].

We have recently reported that *Cyp4a14* knockout male mice, in which elevated testosterone levels drive a marked induction of the Cyp4a12-20-HETE synthase, the sole 20-HETE synthase in mice [20, 21], leading to high tissue and circulating 20-HETE levels, demonstrated a rapid gain of weight on a high fat diet (HFD) when compared to wild type mice [11]. The weight gain in these mice was associated with hyperglycemia, hyperinsulinemia and insulin resistance. Notably, administration of a 20-HETE antagonist attenuated weight gain and prevented the development of insulin resistance [11]. The aforementioned study further supported the notion that 20-HETE has actions on insulin signaling. However, the mechanism by which 20-HETE interferes with insulin signaling and glucose metabolism remains poorly understood.

In the present study, we employed conditional transgenic mice (*Cyp4a12tg*) in which, unlike the male *Cyp4a14* knockout mice, overexpression of Cyp4a12-20-HETE synthase is driven by doxycycline independent of testosterone and is not gender-dependent. Hence, administration of doxycycline to either male or female *Cyp4a12tg* mice induces *Cyp4a12* expression and 20-HETE production within 1-3 days and these levels of expression and production remained as long as doxycycline is present in the drinking water [2, 22]. The present study examines whether acute elevation in 20-HETE levels as in doxycycline-treated *Cyp4a12tg* mice is sufficient to exacerbate weight gain, hyperglycemia and insulin resistance in response to HFD. Here, we report that acute elevation of 20-HETE production is sufficient to exacerbate HFD-driven weight gain and insulin resistance likely by blocking insulin signaling.

MATERIALS AND METHODS

Experimental animals.

All experimental protocols in this study were approved by the New York Medical College Institutional Animal Care and Use Committee (IACUC) in accordance with the National Institutes of Health Guidelines for the Care and Use of Laboratory Animals. The generation and phenotypic characterization of the *Cyp4a12* transgenic (*Cyp4a12tg*) mice in which the expression of the CYP4A12-20-HETE synthase is under the control of an androgen-independent, tetracycline (doxycycline, DOX)-sensitive promoter have been previously described [22]. *Cyp4a12tg* mice (12±1-week-old, 24.2±0.4 g, n=33) were housed in static cages with free access to food and water. Experiments were conducted for 15 weeks. The mice were divided into 6 groups: A) mice fed control diet (CD); B) mice fed a high fat diet (HFD); C) mice fed a HFD and administered the 20-HETE functional antagonist 2,5,8,11,14,17-hexaoxanonadecan-19-yl-20-hydroxyeicosa-6(Z),15(Z)-dienoate (20-SOLA; 10 mg/kg/day in drinking water), which is a PEG-conjugate of 20-6,15-hydroxyeicosadecaenoic acid (20-HEDE), an effective and selective 20-HETE antagonist [23–25]. The indicated dose of 10 mg/kg/day was chosen based on previous studies showing effective antagonism of 20-HETE-mediated effects in vivo [11, 25, 26] : D) mice fed a CD and administered DOX (1 mg/ml) in the drinking water; E) mice fed a HFD and administered DOX (1 mg/ml in drinking water); and F) mice fed a HFD and administered DOX (1 mg/ml) and 20-SOLA (10 mg/kg/day). The control diet (CD) consisted of the following components in amounts represented by percent kilocalories (kcal): Fat – 13.4%; Carbohydrate – 58.0%; Protein – 28.7%. The HFD (Envigo cat.# 03584) consisted of the following components in percent kilocalories: Fat – 58.4%; Carbohydrate – 26.6%; and protein – 15.0%. Approximate fatty acid profile (% total fat): 40% saturated, 50% monounsaturated, 10% polyunsaturated [27]. Food intake, water intake, and body weight were measured weekly. Blood glucose was measured biweekly. Blood pressure and oxygen consumption was measured before and at the end of the experiment.

Blood pressure measurements.

The CODA tail cuff system (Kent Scientific, Torrington, CT) was used to obtain systolic blood pressure. Measurements were collected before and 15 weeks after placing mice on either control or HFD. All animals were allowed to acclimate for 4 days before the first recorded blood pressure measurement. The machine records blood pressure values within ±10% of the average value.

Oxygen consumption.

Mice were acclimated to the oxygen consumption chambers for one hour daily for a week prior to measurements. Oxylet gas analyzer and airflow unit (Oxylet; Panlab-Bioseb, Vitrolles, France) was used for the measurement of oxygen consumption (VO_2) and carbon dioxide production (VCO_2). Recordings were obtained by placing individual mouse in each chamber and flow rate set to maintain dCO_2 between 0.4 and 0.8 ml/min as specified by the manufacturer's instructions. Hourly measurements were performed twice for each mouse. The data for VO_2 are expressed as consumed volume of oxygen per minute per kilogram body weight (ml/min/kg).

Glucose tolerance test and insulin quantification.

Glucose tolerance test was performed at the end of the experiment. Glucose (2 g/kg) was administered by intraperitoneal injection. The tip of the tail was scratched to draw blood. Blood samples were taken at 0, 30, 60, 90, and 120 minutes and glucose measured using Contour blood glucose monitoring system (Bayer). For insulin measurements, blood was collected in capillary tubes, centrifuged at 2,000 RPM for 15 minutes and plasma insulin quantified using the Ultra-Sensitive Mouse Insulin ELISA kit (Crystal Chem., catalog# 90080) according to manufacturer's instruction.

Western Blot.

At the termination of the experiment, mice were sacrificed and tissues were snapped-frozen in liquid nitrogen and stored at −80° C. Tissues were homogenized in lysis buffer containing protease and phosphatase inhibitors. Homogenates were centrifuged and the supernatants were collected and processed for western blot analysis. Samples were loaded onto a 4-20% Mini-PROTEAN TGX precast gel (BioRad). Proteins were then transferred to PVDF membrane via Trans Blot Turbo transfer machine (BioRad). Anti-phospho-IRS-1-Ser307 (2385), Anti-IRS-1 (2382), Anti-IR (3025) and Anti-GAPDH (2118) were purchased from cell signaling technologies. Anti-phospho-IR-Tyr972 (I1783) and Ant-β-actin (A2228) antibody were from Sigma. Anti-CYP4A (sc-271983) was from Santa Cruz Biotechnology. This antibody recognizes all Cyp4a isoforms including Cyp4a10, Cyp4a12 and Cyp4a14. Membranes were incubated overnight with primary antibody followed by secondary antibody and proteins detected using Li-COR odyssey infrared Imaging System (Li-COR, Lincoln NE). Bands were quantified using Odyssey Application Software Version 3.0.21.

LC-MS/MS-based analysis of 20-HETE.

Blood was withdrawn at the end of the experiment by aspiration from the inferior vena cava. Briefly, animals were anesthetized with isoflurane, the abdomen was swabbed with 70% alcohol and opened by a midline longitudinal incision. Next, the caudal (inferior) vena cava was identified, punctured and blood drawn into a heparinized syringe. Blood was centrifuged at 2000 RPM for 15 minutes and plasma samples to which the internal standard (d6 20-HETE) was added were subjected to chloroform/methanol extraction for assessment of 20-HETE. Adipose tissue (abdominal fat) was isolated from mice and incubated in Krebs bicarbonate buffer, pH 7, 1mM NADPH at 37°C for one hour. Tissue incubations were terminated with 2 volumes of cold methanol, d6 20-HETE was added, and samples kept at −80°C. 20-HETE was extracted using solid phase Strata-X Polymeric Reversed Phase 60 mg cartridges (Phenomenex, Torrance, CA) as described [8]. Identification and quantification of 20-HETE were performed on a Shimadzu Triple Quadrupole Mass Spectrometer LCMS-8050 equipped with a Nexera UHPLC using multiple reaction monitoring mode. MS conditions were Ionization mode: Negative heated electrospray (HESI), Applied voltage: −4.5~−3 kV; Nebulizer gas: 3.0 L/min N_2; Drying gas: 5.0 L/min N_2; Heating gas: 12.0 L/min Air; Interface temp: 400°C; DL temp: 100°C; Heat block temp: 500°C. UHPLC conditions: Analytical column: Zorbax Eclipse Plus C18 RRHD (50mm L. X 2.1 mm I.D., 1.8 μm); Mobile phase A: 95% water 5% acetonitrile 0.05% acetic acid; Mobile phase B: Acetonitrile 0.05%; Time program 40% B. (0 min)→75%B. (3 min)→85% B. (7.5 min);

Flow rate: 0.4 mL/min.; Injection volume: 5 μl; Column oven temp: 40C. 20-HETE synthetic standard was used to obtain a standard curve (0.5-500 pg) used to calculate 20-HETE final concentrations. All solvents were HPLC grade or higher.

Cell Culture:

Experiments were performed in differentiated 3T3L1 adipocytes, an established model for *in vitro* screening of insulin sensitivity [28]. Cells were grown in Dulbecco's Modified Eagle's medium (DMEM, VWR Life Sciences) supplemented with 10% FBS until 80% confluence and then differentiated to adipocytes using a standard protocol [29]. Cells were grown in regular growth media to 80% confluence after which they incubated in a serum-free growth medium for 8 hours and washed 3 times with phosphate buffered saline (PBS, pH 7.4). Cells were treated with 20-HETE (10 nM) in the presence or absence of the 20-HETE receptor antagonist sodium ((6Z,15Z)-N-(20-hydroxyeicosa-6(Z),15(Z)-dienoyl)aspartate) (AAA, 10 nM) [30, 31] in a serum-free low-glucose (1g/l) DMEM for 5 minutes followed by stimulation with insulin (20 nM) for 10 minutes after which supernatant was removed and cells scraped in ice-cold RIPA buffer with protease and phosphatase inhibitors. Cell lysate proteins were quantified using the Bradford reagent.

Statistical analysis.

All data are expressed in terms of Means ± SE. Significance of difference in mean values was determined using one-way ANOVA or repeated measures two-way ANOVA, followed by Tukey's *post hoc* multiple comparison test. $P<0.05$ was considered to be significant.

RESULTS

HFD-driven weight gain is amplified following induction of the Cyp4a12-20-HETE synthase

Body weight of mice at the start of the 15-week experiment was not significantly different among all groups and averaged 24.2±0.4 g (n=33) (Figure 1A). As seen in Figure 1A, body weight markedly increased in all groups on a HFD ($p<0.0001$), while the mice on CD treated with (3.75±0.60 g; $p=0.93$) and without (2.35±0.46 g; $p=0.99$) DOX showed no significant body weight increase over the 15-week feeding period. DOX-treated *Cyp4a12tg* mice fed a HFD showed a rapid and significant gain in body weight compared to DOX-treated mice on a CD (20.63±2.9 vs. 3.75±0.6 g, $p<0.0001$) (Figure 1B). Notably, the weight gain of DOX-treated HFD-fed *Cyp4a12tg* mice was significantly greater than mice fed a HFD without DOX (20.63±2.9 vs. 13.51±0.94 g, $p<0.001$). Administration of 20-SOLA, a selective 20-HETE antagonist, significantly attenuated weight gain in DOX+HFD-fed mice (11.37±1.78 vs. 20.63±2.9 g, $p<0.001$; Figure-1B). The effect of 20-SOLA on weight gain in DOX +HFD-fed mice was evident from week-9 ($p<0.05$) and persisted up to week-15 (Figure 1A). In contrast, body weight-gain of *Cyp4a12tg* mice fed HFD alone and treated with 20-SOLA was not different than the untreated mice (Figure 1A & 1B), indicating that the effect of 20-SOLA on attenuation of HFD-induced body weight-gain is 20-HETE-dependent.

During the time of HFD feeding, food and water intake was not different among all experimental groups. As seen in Figure 2A, the weekly average of energy intake was not different between groups and ranged between 98.37±0.26 kcal/week in the vehicle groups

and 94.05±51.23 kcal/week in the DOX-treated groups. This indicates that 20-HETE-dependent accelerated weight gain on HFD-feeding is not associated with alterations in food intake.

Oxygen consumption, a measure of energy expenditure, was significantly reduced in *Cyp4a12tg* mice fed DOX+HFD compare to the corresponding mice fed HFD alone ($p<0.001$), indicating a decreased metabolism (Figure 2B). Administration of 20-SOLA prevented HFD-mediated decrease in oxygen consumption in DOX+HFD-fed *Cyp4a12tg* mice (69.84±1.82 vs 50.17±2.9 ml/min/kg, $p<0.05$), suggesting the effect of 20-SOLA may be related to attenuation of 20-HETE mediated HFD-induced decrease in metabolism.

Increased blood pressure (BP) is a feature of DOX-treated *Cyp4a12tg* mice. Hence, administration of DOX alone increased ($p<0.001$) systolic blood pressure, indicating a hypertensive phenotype as previously reported [22, 32]. HFD feeding alone increased blood pressure from 109±5 to 123±1 mmHg ($p<0.05$). However, addition of DOX to HFD resulted in a further increase in systolic BP compared to HFD alone (153±5.11 mmHg, $p<0.0001$) or DOX alone (135.2±5.48, $p<0.05$) (Figure 2C). As expected, 20-SOLA administration significantly reduced blood pressure of DOX+HFD-fed mice (118.34±5.4 vs. 153.4±5.11 mmHg, $p<0.0001$). 20-SOLA did not affect the BP of *Cyp4a12tg* mice fed a HFD without DOX (Figure 2C).

Induction of Cyp4a12-20-HETE synthase and HFD results in hyperglycemia, hyperinsulinemia and impaired glucose tolerance

As seen in Figure 3A, fasting blood glucose at the end of the 15-weeks study was unchanged in *Cyp4a12tg* mice on either CD (109.2±5.3 mg/dl) or HFD (110.1±3.6 mg/dl), nor did it change when mice were placed on CD+DOX (101.2±6.1). However, *Cyp4a12tg* mice fed HFD+DOX for 15 weeks were hyperglycemic compared to those fed CD+DOX or HFD alone (144.0±3.5 mg/dl; $p<0.01$). The increase in fasting glucose in the DOX+HFD group was likely due to increased 20-HETE levels since it was prevented by administration of the 20-HETE antagonist, 20-SOLA (104.2±9.2 mg/dl; $p<0.001$ vs DOX+HFD). 20-SOLA had no effect on fasting glucose levels in mice fed HFD alone.

Plasma insulin levels measured at the end of the 15-week study were 5-fold higher in mice fed HFD+DOX than mice fed HFD alone ($p<0.0001$) (Figure 3B). Feeding HFD alone for 15-weeks had no significant effect on insulin levels and remained similar to levels measured in mice on CD or CD+DOX (0.53±0.06 and 0.55±0.10 ng/ml, respectively). 20-HETE blockade *via* 20-SOLA administration lowered serum insulin levels (0.71±0.09 ng/ml, $p<0.001$) of DOX+HFD-fed mice. In the absence of DOX administration, 20-SOLA treatment did not affect plasma insulin levels of HFD fed Cyp4a12tg mice.

To assess the ability of these animals to metabolize glucose, an intraperitoneal glucose tolerance test was performed at the end of the 15-week study. *Cyp4a12tg* mice fed DOX +HFD showed a significant ($p<0.0001$) impairment of glucose tolerance and blood glucose levels were not normalized at the end of two-hour period (Figure 4A). This is also evident from the assessment of area under the curve (AUC) (Figure 4B). In the absence of DOX, HFD feeding did not result in an impairment of glucose tolerance in the *Cyp4a12tg* mice.

Glucose-stimulated insulin secretion was also significantly elevated during the entire course of GTT in Cyp4a12tg mice fed DOX+HFD (Figure 4C). This is also reflected in AUC-insulin data, indicative of insulin resistance (Figure 4D). The impaired glucose tolerance in DOX+HFD-fed *Cyp4a12tg* mice was significantly improved by 20-SOLA administration with blood glucose values being normalized after 2 hours of intraperitoneal glucose tolerance (Figure 4A). Glucose stimulated insulin secretion (GSIS), indicated by plasma insulin levels measured after an intraperitoneal glucose challenge, were significantly lower after 20-SOLA treatment in the DOX+HFD fed Cyp4a12tg mice (Figure 4C). This indicator of improved insulin resistance is also reflected by AUC-insulin data.

20-SOLA administration in *Cyp4a12tg* mice fed HFD without DOX did not affect blood glucose levels and plasma insulin levels during glucose tolerance test, suggesting that induction of the *Cyp4a12* expression and the associated increase in 20-HETE levels are critical to the development of insulin resistance in response to HFD. To this end, 20-HETE levels in plasma and visceral fat increased in response to DOX and HFD (Figure 5A and B). As expected, administration of DOX along with a control diet did result in a significant increase in adipose and plasma levels of 20-HETE. Feeding of a HFD together with DOX resulted in a further 2-fold increase in 20-HETE levels. However, in the absence of DOX, HFD-fed animals did not show change in plasma and adipose 20-HETE levels compared to CD-fed animals. Elevated levels of plasma and adipose tissue 20-HETE in DOX+HFD fed *Cyp4a12tg* mice were not affected by administration of the 20-HETE antagonist 20-SOLA, which blocks the actions of 20-HETE.

The increase of 20-HETE levels was likely due to the DOX-driven induction of the *Cyp4a12* transgene. Cyp4a12 protein levels increased in adipose tissue (Figure 5C) and skeletal muscle (Figure 5D) from all groups that were given DOX either on CD or HFD. However, the increase in Cyp4a12 protein levels was greater in response to HFD+DOX as compared to CD+DOX. This is in agreement with reports indicating that a HFD results in a dramatic induction of *Cyp4A* genes, which in rodents is mediated through activation of PPARα [33, 34].

HFD induces impairment of insulin receptor signaling in a 20-HETE-dependent manner

Our results indicate that diet-induced insulin resistance in transgenic mice overexpressing Cyp4a12–20-HETE synthase is prevented by 20-SOLA. This raises the possibility that 20-HETE may interfere with insulin action. We examined the impact of HFD and overproduction of 20-HETE on key markers of insulin signaling including phosphorylation of the insulin receptor (IR) and insulin receptor substrate-1 (IRS-1) in tissues that are primary targets of insulin action, i.e., adipose tissue, skeletal muscle and liver. In the *Cyp4a12tg* mice where DOX was administered to overexpress Cyp4a12–20-HETE, HFD feeding resulted in a significant 40, 70 and 60% reduction in phosphorylation of insulin receptor at Tyr-972 in skeletal muscle, adipose tissue and liver, respectively (Figure 6). Administration of 20-SOLA, a 20-HETE functional antagonist, significantly attenuated the HFD-mediated decrease in the level of P-IR-Tyr972 in skeletal muscle, adipose tissue and liver of *Cyp4a12tg* mice. Phosphorylation of insulin receptor at Tyr-972 (p-IR^{Y972}) is an

indicator of receptor activation and a decrease in phosphorylation is associated with insulin resistance.

The adaptor protein, IRS-1, is phosphorylated by the insulin receptor at specific tyrosine residues and signals to downstream pathways. Phosphorylation of IRS-1 at Ser307 results in its inactivation and degradation. This inhibits insulin receptor signal transduction and contributes to peripheral insulin resistance [35]. In *Cyp4a12tg* mice, DOX+HFD feeding was associated with a 3-, 3- and 4-fold increase in inhibitory phosphorylation of IRS-1 at Ser307 in skeletal muscle, adipose tissue and liver, respectively (Figure 7). Moreover, DOX +HFD-fed *Cyp4a12tg* mice also had a 30, 40 and 30% decrease in levels of IRS-1 suggesting an accelerated degradation occurring as a result of its Ser-307 phosphorylation. The reduced IRS-1 levels are indicative of down-regulated insulin signaling pathway and peripheral insulin resistance. Importantly, treatment with 20-SOLA prevented the HFD-induced increase in inhibitory Ser307 phosphorylation of IRS-1 in the skeletal muscle, adipose tissue and liver of DOX-treated *Cyp4a12tg* mice. Moreover, 20-SOLA prevented HFD-induced decrease in IRS-1 levels indicative of reduction in degradation.

20-HETE inhibits insulin stimulated tyrosine phosphorylation of the insulin receptor

The findings that insulin signaling was greatly impaired in DOX-treated HFD-fed *Cyp4a12tg* mice and that 20-SOLA prevented this impairment suggested that 20-HETE directly affect insulin signaling. To this end, we used differentiated 3T3L1 adipocytes which is an established model for *in vitro* screening of insulin sensitivity and have abundant expression of the insulin receptor and its downstream signaling partners [28]. As seen in Figure 8, treatment of differentiated 3T3L1 adipocytes with 20-HETE (10 nM) for 5 minutes resulted in a marked inhibition of insulin (10 nM)-mediated phosphorylation of its receptor at Tyr972 (4.64±0.47 vs 2.04±0.23-fold change, $p<0.05$). This effect was not seen in the presence of AAA, a 20-HETE receptor antagonist (an analog of 20-SOLA) [30, 31], indicating that the inhibition of Tyr-972 phosphorylation of the insulin receptor was driven by 20-HETE (Figure 8).

DISCUSSION

Studies in humans and animal models implied a link between 20-HETE levels, obesity (BMI) and insulin resistance [3–6, 8, 11, 36]. In addition, cell culture studies suggested that 20-HETE affects insulin receptor and downstream signaling as well as glucose-stimulated insulin secretion [18, 19, 37]. This together with the known inducing action of diet rich in fat on Cyp4a isoforms [33], among which the Cyp4a12 is the sole murine 20-HETE producing enzyme [21], enforces the notion that 20-HETE plays an important role in the development and/or progression of obesity-driven metabolic dysfunction. Key findings in this study provide additional evidence for this notion.

The first key finding is that HFD-driven weight gain is magnified by acute elevation of 20-HETE production. The animal model employed in this study is a conditional overexpression of the Cyp4a12–20-HETE synthase that is transcriptionally activated by DOX. Data showing increased tissue expression of Cyp4a12 and levels of 20-HETE in response to DOX validated this model. We have previously shown that in the *Cyp4a14* knockout mice, a

model of androgen-mediated Cyp4a12-driven 20-HETE overproduction, HFD feeding resulted in an accelerated weight-gain and development of insulin resistance [11]. Unlike the *Cyp4a14* knockout mice, the *Cyp4a12tg* mice offers an advantage of studying 20-HETE overproduction in an inducible and androgen-independent setting. Moreover, this model allows a built-in control group in which Cyp4a12-20-HETE synthase is not activated and therefore a better assessment of the contribution of 20-HETE to the development of HFD-driven hyperglycemia and insulin resistance. While all groups gained significant weight when placed on HFD, the mice given DOX gained twice as much. This excess weight gain was clearly 20-HETE-mediated since it was completely negated by administration of 20-SOLA. The contribution of 20-HETE to weight gain was significantly manifested from weeks 7-8 of HFD+DOX feeding, suggesting that a certain threshold level or accumulating amounts of 20-HETE needs to be achieved before it has an effect. Importantly, the difference in weight gain between the groups was not the consequence of difference in food/energy intake but rather a difference in energy expenditure. Recent studies suggested that 20-HETE affects metabolism by interfering with mitochondrial function [11, 38], which may account for the reduction in energy expenditure in the HFD+DOX group.

Since DOX-driven transcriptional activation of Cyp4a12-20-HETE synthase in the *Cyp4a12tg* mice results in hypertension, it is important to consider the possible contribution of 20-HETE-dependent hypertension to development of insulin resistance. The co-existence of insulin resistance and hypertension is a common feature of metabolic syndrome. However, it is unclear whether this is a cause-effect relationship or a non-causal association [39, 40]. Insulin can raise blood pressure through mechanisms involving increased renal sodium reabsorption, activation of the sympathetic nervous system, alteration of transmembrane ion transport, and hypertrophy of resistance vessels [41]. Conversely, hypertension can lead to insulin resistance by affecting the delivery of insulin and glucose to skeletal muscle cells, resulting in impaired glucose uptake. Our results indicated that hyperglycemia and insulin resistance only occurred when HFD and DOX (induction of *Cyp4a12* and over-production of 20-HETE) are combined. While we cannot exclude the possibility that the hypertension-driven by 20-HETE is a driving force of HFD-induced hyperglycemia and insulin resistance, it is evident from the effect of 20-SOLA and the *in vitro* studies that 20-HETE interferes with insulin signaling and therefore may be a contributing factor as well.

The second key finding is that 20-HETE is the driving force of hyperglycemia and insulin resistance in response to HFD. A 15-week diet that is rich in fat alone did not result in hyperglycemia and insulin resistance. The only group that developed hyperglycemia and insulin resistance within this time frame was the one receiving HFD+DOX, suggesting that 20-HETE is probably the cause. This notion is further supported by the fact that administration of 20-SOLA, an effective antagonist of 20-HETE actions, abrogated the HFD +DOX effect. These results suggest that 20-HETE acts as a second hit by adding distinct actions on mechanisms regulating glucose homeostasis. To this end, tissues that are primary targets of insulin action including skeletal muscle, adipose tissue and liver from mice fed HFD+DOX displayed a marked 50-70% reduction in tyrosine 972 phosphorylation of the insulin receptor, the initial step of insulin signaling towards increasing glucose uptake. This reduction in insulin receptor phosphorylation was associated with inactivation of IRS-1 as

evidenced by an increase in its serine 307 phosphorylation [35] in tissues from the DOX +HFD group. The ability of 20-SOLA to completely abolish the HFD+DOX provided strong evidence that 20-HETE mediates this impaired insulin signaling, which brings us to the third key finding.

There are a few reports demonstrating the ability of 20-HETE to interfere with glucose homeostasis and insulin signaling and function. Studies by Zhang et al [37] and Lai et al [12] found that mice overexpressing the human CYP4F2-20-HETE synthase develop hyperglycemia and suggested that it is, in part, the result of 20-HETE's ability to attenuate glucose-stimulated insulin secretion. On the other hand, Tunaru et al [19] showed that 20-HETE promotes glucose-stimulated insulin secretion. Another study in endothelial cells has demonstrated that 20-HETE impairs insulin signaling by promoting phosphorylation of IRS-1 on Ser-616 [18]. Our recent study also suggested that 20-HETE negatively affect insulin signaling [11]. The mechanism by which 20-HETE impairs insulin function is largely unclear. However, the current study suggests that in differentiated 3T3 adipocytes, it inhibits insulin receptor phosphorylation by activating its receptor GPR75. This finding is substantiated by the fact that blocking the receptor with an antagonist prevented 20-HETE's ability to inhibit insulin receptor tyrosine phosphorylation. We postulated that binding of 20-HETE to GPR75 (a Gq protein-coupled receptor) stimulates the IP3/DAG signaling cascade that further, via increased intracellular Ca^{2+}, activates PKCα to stimulate phosphatases responsible for dephosphorylation of the insulin receptor. Activation of PKC signaling by 20-HETE has been shown in arterial preparations and cardiomyocytes [42–44]. However, the cellular target of 20-HETE has not been identified. We have identified GPR75 as 20-HETE's receptor and shown that 20-HETE-GPR75 pairings activates a Gqa-mediated IP3 and PKC signaling in endothelial and smooth muscle cells [2]. A recent study in prostate cancer cells also suggested that 20-HETE-GPR75 pairing leads to PKCα activation and signaling [30]. The current study implies that GPR75 may be an important target for the regulation of insulin function and additional studies need to be performed to support this notion.

In summary, findings in this study implicate 20-HETE as a key determinant in the development of obesity-driven insulin resistance. Hence, the combination of high levels of 20-HETE along with HFD is necessary to establish this phenotype. It is worth noting that high level of circulating 20-HETE is associated with obesity in humans and in animal models of obesity and metabolic syndrome. This high level of 20-HETE might be, at least in part, promotes and maintains a state of insulin resistance and metabolic pathology.

Acknowledgements

We wish to thank the Shimadzu LC-MS/MS Lipidomics core and Dr. Lars Bellner for his assistance in measuring 20-HETE. We also would like to thank Dr. Varunkumar Pandey for his important contribution to this study.

Funding

This work was supported by grants from the National Institutes of Health grants PO1034300 and RO1HL139793 (MLS), diversity supplement to Victor Garcia HL139793-1S, and by the Robert A. Welch Foundation (I-0011) (JRF).

REFERENCES

[1]. Rocic P, and Schwartzman ML. 20-HETE in the regulation of vascular and cardiac function. Pharmacology & therapeutics, 2018.

[2]. Garcia V, Gilani A, Shkolnik B, Pandey V, Zhang FF, Dakarapu R, et al. 20-HETE Signals Through G-Protein-Coupled Receptor GPR75 (Gq) to Affect Vascular Function and Trigger Hypertension. Circ Res 120(11):1776–88, 2017. [PubMed: 28325781]

[3]. Issan Y, Hochhauser E, Guo A, Gotlinger KH, Kornowski R, Leshem-Lev D, et al. Elevated level of pro-inflammatory eicosanoids and EPC dysfunction in diabetic patients with cardiac ischemia. Prostaglandins Other Lipid Mediat 100–101:15–21, 2013.

[4]. Peterson SJ, Vanella L, Gotlinger K, Jiang H, Singh SP, Sodhi K, et al. Oxidized HDL is a potent inducer of adipogenesis and causes activation of the Ang-II and 20-HETE systems in human obese females. Prostaglandins Other Lipid Mediat 123:68–77, 2016. [PubMed: 27179555]

[5]. Tsai IJ, Croft KD, Mori TA, Falck JR, Beilin LJ, Puddey IB, et al. 20-HETE and F2-isoprostanes in the metabolic syndrome: the effect of weight reduction. Free Radic Biol Med 46(2):263–70, 2009. [PubMed: 19013235]

[6]. Ward NC, Hodgson JM, Puddey IB, Beilin LJ, and Croft KD. 20-Hydroxyeicosatetraenoic acid is not associated with circulating insulin in lean to overweight humans. Diabetes Res Clin Pract 74(2):197–200, 2006. [PubMed: 16713008]

[7]. Gervasini G, Luna E, Garcia-Cerrada M, Garcia-Pino G, and Cubero JJ. Risk factors for post-transplant diabetes mellitus in renal transplant: Role of genetic variability in the CYP450-mediated arachidonic acid metabolism. Mol Cell Endocrinol 419:158–64, 2016. [PubMed: 26483195]

[8]. Joseph G, Soler A, Hutcheson R, Hunter I, Bradford C, Hutcheson B, et al. Elevated 20-HETE impairs coronary collateral growth in metabolic syndrome via endothelial dysfunction. Am J Physiol Heart Circ Physiol 312(3):H528–H40, 2017. [PubMed: 28011587]

[9]. Soler A, Hunter I, Joseph G, Hutcheson R, Hutcheson B, Yang J, et al. Elevated 20-HETE in metabolic syndrome regulates arterial stiffness and systolic hypertension via MMP12 activation. Journal of molecular and cellular cardiology 117:88–99, 2018. [PubMed: 29428638]

[10]. Theken KN, Deng Y, Schuck RN, Oni-Orisan A, Miller TM, Kannon MA, et al. Enalapril reverses high-fat diet-induced alterations in cytochrome P450-mediated eicosanoid metabolism. Am J Physiol Endocrinol Metab 302(5):E500–9, 2012. [PubMed: 22185841]

[11]. Gilani A, Pandey V, Garcia V, Agostinucci K, Singh SP, Schragenheim J, et al. High-fat diet-induced obesity and insulin resistance in CYP4a14(−/−) mice is mediated by 20-HETE. Am J Physiol Regul Integr Comp Physiol 315(5):R934–r44, 2018. [PubMed: 30088983]

[12]. Lai G, Wu J, Liu X, and Zhao Y. 20-HETE induces hyperglycemia through the cAMP/PKA-PhK-GP pathway. Mol Endocrinol 26(11):1907–16, 2012. [PubMed: 22918876]

[13]. Wang Z, Yadav AS, Leskova W, and Harris NR. Inhibition of 20-HETE attenuates diabetes-induced decreases in retinal hemodynamics. Experimental eye research 93(1):108–13, 2011. [PubMed: 21658386]

[14]. Eid S, Maalouf R, Jaffa AA, Nassif J, Hamdy A, Rashid A, et al. 20-HETE and EETs in diabetic nephropathy: a novel mechanistic pathway. PloS one 8(8):e70029, 2013. [PubMed: 23936373]

[15]. Yousif MH, Benter IF, Dunn KM, Dahly-Vernon AJ, Akhtar S, and Roman RJ. Role of 20-hydroxyeicosatetraenoic acid in altering vascular reactivity in diabetes. Auton Autacoid Pharmacol 29(1–2):1–12, 2009. [PubMed: 19302551]

[16]. Luo P, Zhou Y, Chang HH, Zhang J, Seki T, Wang CY, et al. Glomerular 20-HETE, EETs, and TGF-beta1 in diabetic nephropathy. Am J Physiol Renal Physiol 296(3):F556–63, 2009. [PubMed: 19129258]

[17]. Kim DH, Puri N, Sodhi K, Falck JR, Abraham NG, Shapiro J, et al. Cyclooxygenase-2 dependent metabolism of 20-HETE increases adiposity and adipocyte enlargement in mesenchymal stem cell-derived adipocytes. Journal of lipid research 54(3):786–93, 2013. [PubMed: 23293373]

[18]. Li X, Zhao G, Ma B, Li R, Hong J, Liu S, et al. 20-Hydroxyeicosatetraenoic acid impairs endothelial insulin signaling by inducing phosphorylation of the insulin receptor substrate-1 at Ser616. PloS one 9(4):e95841, 2014. [PubMed: 24763529]

[19]. Tunaru S, Bonnavion R, Brandenburger I, Preussner J, Thomas D, Scholich K, et al. 20-HETE promotes glucose-stimulated insulin secretion in an autocrine manner through FFAR1. Nature communications 9(1):177, 2018.

[20]. Holla VR, Adas F, Imig JD, Zhao X, Price E, Jr., Olsen N, et al. Alterations in the regulation of androgen-sensitive Cyp 4a monooxygenases cause hypertension. Proc Natl Acad Sci U S A 98(9):5211–6, 2001. [PubMed: 11320253]

[21]. Muller DN, Schmidt C, Barbosa-Sicard E, Wellner M, Gross V, Hercule H, et al. Mouse Cyp4a isoforms: enzymatic properties, gender- and strain-specific expression, and role in renal 20-hydroxyeicosatetraenoic acid formation. The Biochemical journal 403(1):109–18, 2007. [PubMed: 17112342]

[22]. Wu CC, Mei S, Cheng J, Ding Y, Weidenhammer A, Garcia V, et al. Androgen-sensitive hypertension associates with upregulated vascular CYP4A12-20-HETE synthase. J Am Soc Nephrol 24(8):1288–96, 2013. [PubMed: 23641057]

[23]. Alonso-Galicia M, Falck JR, Reddy KM, and Roman RJ. 20-HETE agonists and antagonists in the renal circulation. Am J Physiol 277(5 Pt 2):F790–6, 1999. [PubMed: 10564244]

[24]. Ding Y, Wu CC, Garcia V, Dimitrova I, Weidenhammer A, Joseph G, et al. 20-HETE induces remodeling of renal resistance arteries independent of blood pressure elevation in hypertension. Am J Physiol Renal Physiol 305(5):F753–63, 2013. [PubMed: 23825080]

[25]. Pandey V, Garcia V, Gilani A, Mishra P, Zhang FF, Paudyal MP, et al. The Blood Pressure-Lowering Effect of 20-HETE Blockade in Cyp4a14(−/−) Mice Is Associated with Natriuresis. J Pharmacol Exp Ther 363(3):412–8, 2017. [PubMed: 28912346]

[26]. Gangadhariah MH, Luther JM, Garcia V, Paueksakon P, Zhang MZ, Hayward SW, et al. Hypertension is a major contributor to 20-hydroxyeicosatetraenoic acid-mediated kidney injury in diabetic nephropathy. J Am Soc Nephrol 26(3):597–610, 2015. [PubMed: 25071086]

[27]. Molnar J, Yu S, Mzhavia N, Pau C, Chereshnev I, and Dansky HM. Diabetes induces endothelial dysfunction but does not increase neointimal formation in high-fat diet fed C57BL/6J mice. Circ Res 96(11):1178–84, 2005. [PubMed: 15879311]

[28]. Rubin CS, Hirsch A, Fung C, and Rosen OM. Development of hormone receptors and hormonal responsiveness in vitro. Insulin receptors and insulin sensitivity in the preadipocyte and adipocyte forms of 3T3-L1 cells. J Biol Chem 253(20):7570–8, 1978. [PubMed: 81205]

[29]. Zebisch K, Voigt V, Wabitsch M, and Brandsch M. Protocol for effective differentiation of 3T3-L1 cells to adipocytes. Analytical biochemistry 425(1):88–90, 2012. [PubMed: 22425542]

[30]. Cardenas S, Colombero C, Panelo L, Dakarapu R, Falck John R, Costas Monica A, et al. GPR75 receptor mediates 20-HETE-signaling and metastatic features of androgen-insensitive prostate cancer cells. Biochimica et biophysica acta Molecular and cell biology of lipids 1865:158573–80, 2019. [PubMed: 31760076]

[31]. Gawrys O, Husková Z, Baranowska I, Walkowska A, Sadowski J, Kikerlová S, et al. Combined treatment with epoxyeicosatrienoic acid analog and 20-hydroxyeicosatetraenoic acid antagonist provides substantial hypotensive effect in spontaneously hypertensive rats. Journal of hypertension 38(9):1802–10, 2020. [PubMed: 32384390]

[32]. Garcia V, Joseph G, Shkolnik B, Ding Y, Zhang FF, Gotlinger K, et al. Angiotensin II receptor blockade or deletion of vascular endothelial ACE does not prevent vascular dysfunction and remodeling in 20-HETE-dependent hypertension. Am J Physiol Regul Integr Comp Physiol 309(1):R71–8, 2015. [PubMed: 25924878]

[33]. Hardwick JP. Cytochrome P450 omega hydroxylase (CYP4) function in fatty acid metabolism and metabolic diseases. Biochemical pharmacology 75(12):2263–75, 2008. [PubMed: 18433732]

[34]. Hardwick JP, Eckman K, Lee YK, Abdelmegeed MA, Esterle A, Chilian WM, et al. Eicosanoids in metabolic syndrome. Advances in pharmacology (San Diego, Calif) 66:157–266, 2013.

[35]. Gual P, Le Marchand-Brustel Y, and Tanti JF. Positive and negative regulation of insulin signaling through IRS-1 phosphorylation. Biochimie 87(1):99–109, 2005. [PubMed: 15733744]

[36]. Ronquillo MD, Mellnyk A, Cardenas-Rodriguez N, Martinez E, Comoto DA, Carmona-Aparicio L, et al. Different gene expression profiles in subcutaneous & visceral adipose tissues from Mexican patients with obesity. The Indian journal of medical research 149(5):616–26, 2019. [PubMed: 31417029]

[37]. Zhang B, Lai G, Wu J, Sun R, Xu R, Yang X, et al. 20-HETE attenuates the response of glucose-stimulated insulin secretion through the AKT/GSK-3beta/Glut2 pathway. Endocrine 54(2):371–82, 2016. [PubMed: 27568038]

[38]. Lakhkar A, Dhagia V, Joshi SR, Gotlinger KH, Patel D, Sun D, et al. 20-HETE-Induced Mitochondrial Superoxide and Inflammatory Phenotype in Vascular Smooth Muscle is Prevented by Glucose-6-Phosphate Dehydrogenase Inhibition. Am J Physiol Heart Circ Physiol 310(9):H1107–17, 2016. [PubMed: 26921441]

[39]. Salvetti A, Brogi G, Di Legge V, and Bernini GP. The inter-relationship between insulin resistance and hypertension. Drugs 46 Suppl 2:149–59, 1993. [PubMed: 7512468]

[40]. Hu FB, and Stampfer MJ. Insulin resistance and hypertension: the chicken-egg question revisited. Circulation 112(12):1678–80, 2005. [PubMed: 16172279]

[41]. Horita S, Seki G, Yamada H, Suzuki M, Koike K, and Fujita T. Insulin resistance, obesity, hypertension, and renal sodium transport. Int J Hypertens 2011:391762, 2011. [PubMed: 21629870]

[42]. Nakayama K, Obara K, Tanabe Y, and Ishikawa T. 20-Hydroxyeicosatetraenoic acid potentiates contractile activation of canine basilar artery in response to stretch via protein kinase Calpha-mediated inhibition of calcium-activated potassium channel. Advances in experimental medicine and biology 538:411–6; discussion 6, 2003. [PubMed: 15098687]

[43]. Sun CW, Falck JR, Harder DR, and Roman RJ. Role of tyrosine kinase and PKC in the vasoconstrictor response to 20-HETE in renal arterioles. Hypertension 33(1 Pt 2):414–8, 1999. [PubMed: 9931139]

[44]. Zeng Q, Han Y, Bao Y, Li W, Li X, Shen X, et al. 20-HETE increases NADPH oxidase-derived ROS production and stimulates the L-type Ca2+ channel via a PKC-dependent mechanism in cardiomyocytes. Am J Physiol Heart Circ Physiol 299(4):H1109–17, 2010. [PubMed: 20675568]

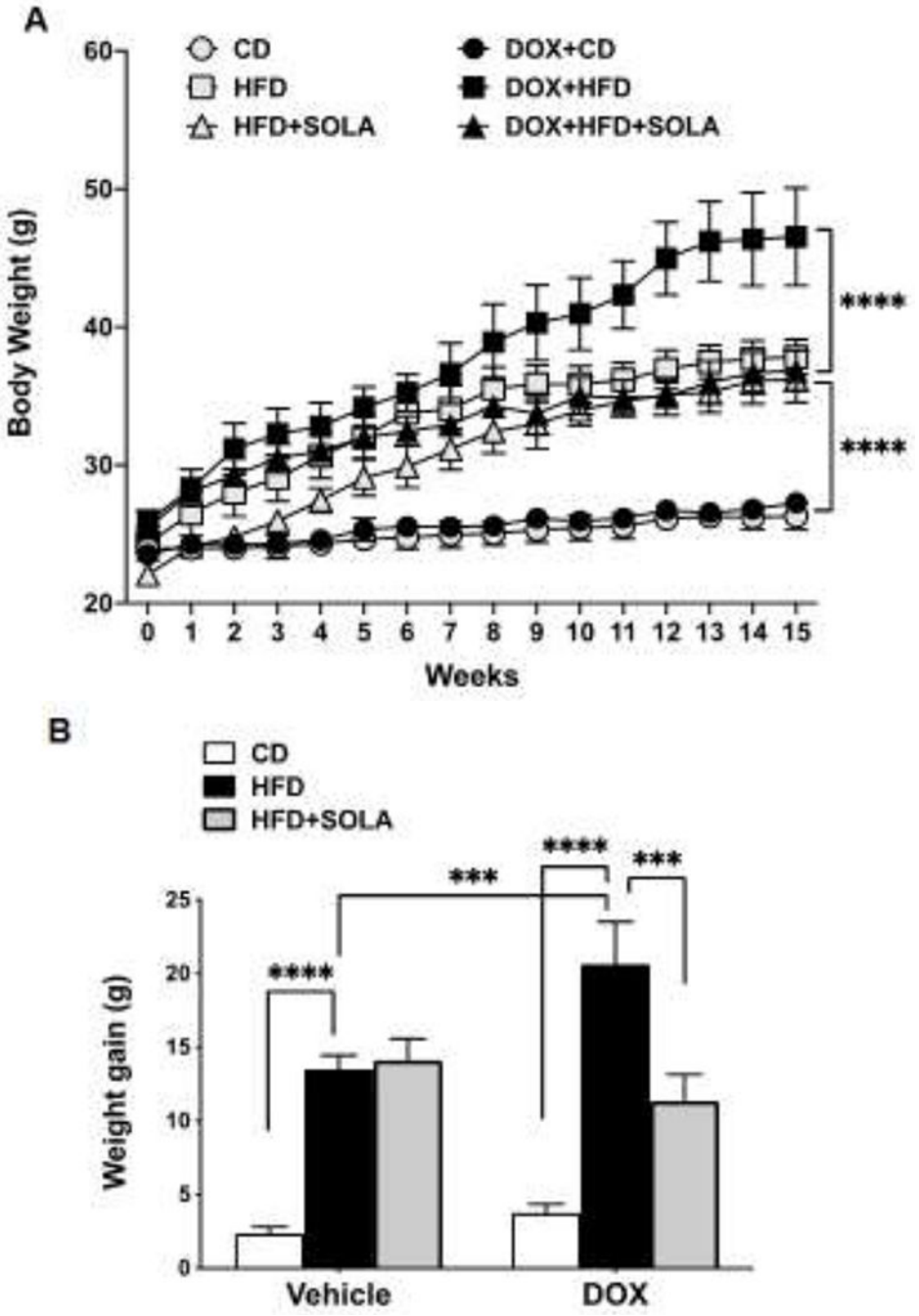

Figure 1:

(A) Body weight over a period of 15 weeks of feeding high fat diet (HFD) or control diet (CD), with or without supplementation of doxycycline (DOX) to induce Cyp4a12 overexpression and/or 20-SOLA, a selective 20-HETE antagonist. (B) Cumulative body weight gain post 15 weeks on respective diet feeding (n=6-8 per group); ****p<0.001* *****p<0.0001 using repeated-measures two-way ANOVA with post-hoc Tukey's test.*

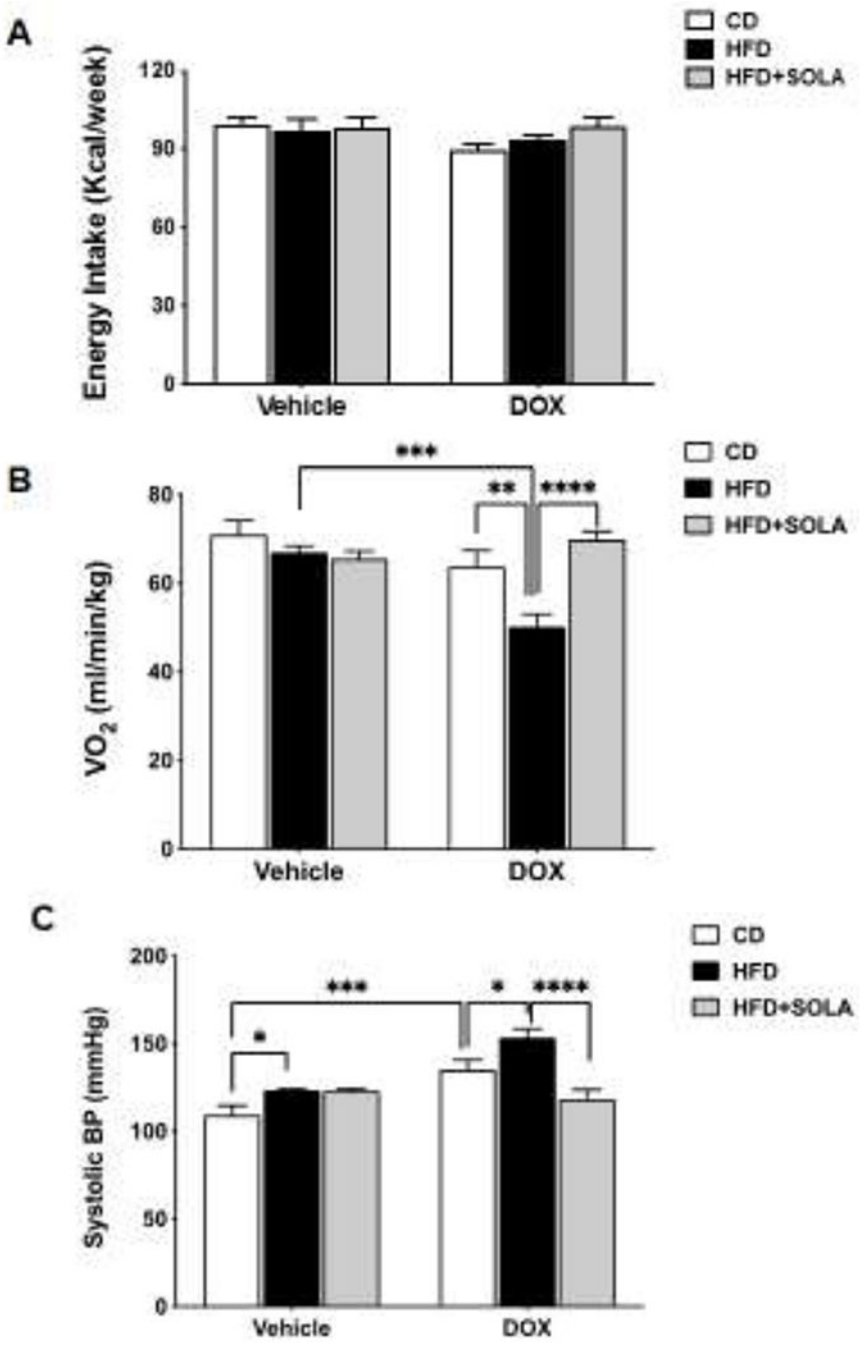

Figure 2:

(A) Average weekly energy intake in kilocalories consumed per week (B) Oxygen consumption in milliliters per minute per kilogram body weight post 15 weeks of respective diet feeding (C) Systolic Blood Pressure post 15 weeks of respective diet feeding (n=5-8 per group); CD, Control diet; HFD, High fat diet; DOX, Doxycycline; SOLA, 20-HETE antagonist; **p<0.05*, ***P<0.01*, ****p<0.001*, *****p<0.0001 using two-way ANOVA with post-hoc Tukey's test.*

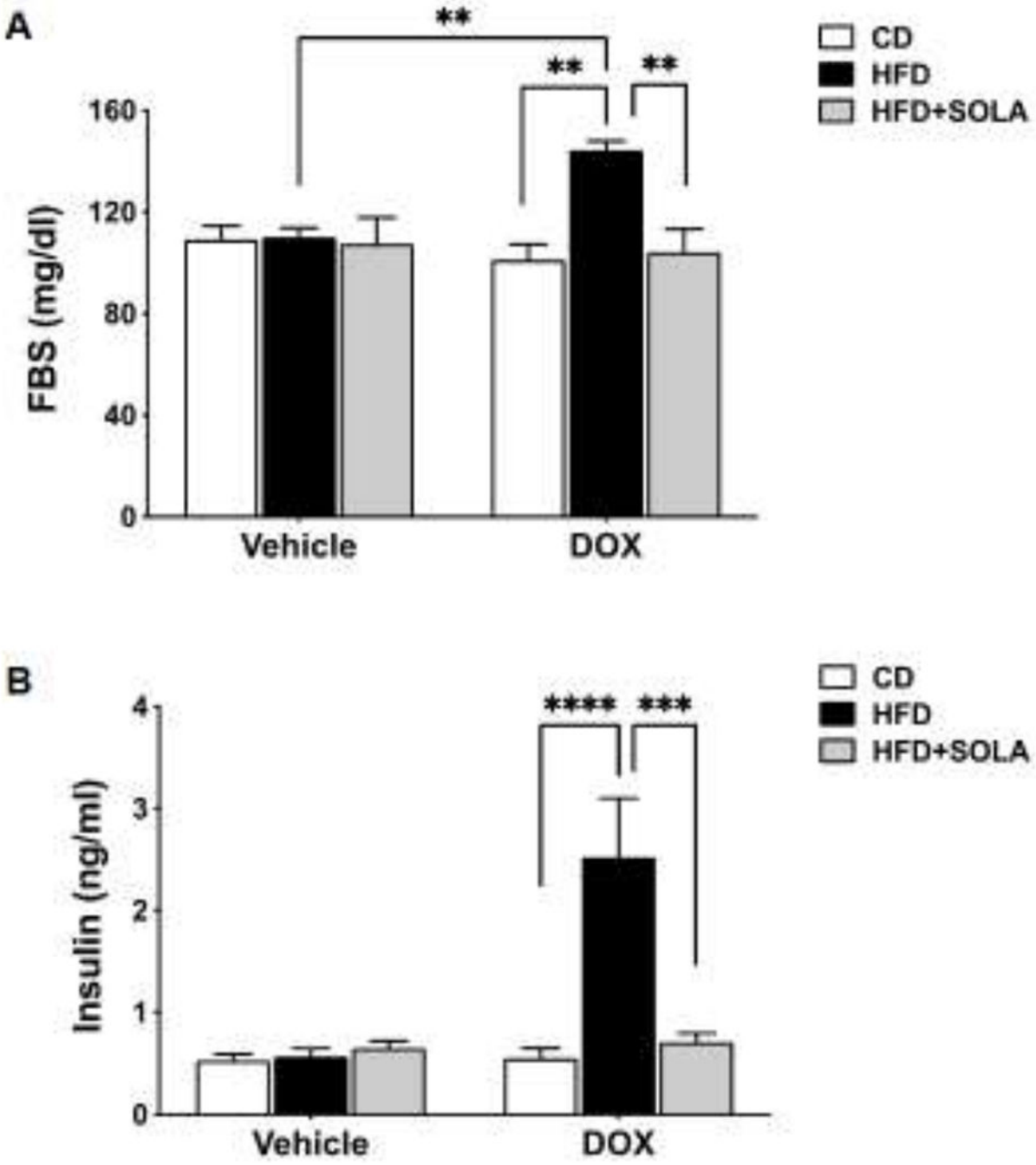

Figure 3:

(A) Fasting blood glucose and (B) Plasma insulin levels measured post 15 weeks of respective diet feeding. Blood glucose was measured using commercial finger-stick glucose meter and plasma insulin was measured using ultra-sensitive mouse insulin ELIZA kit. (n=5-8 per group); CD, Control diet; HFD, High fat diet; DOX, Doxycycline; SOLA, 20-HETE antagonist; ** *P<0.01*, *** *p<0.001*, **** *p<0.0001 based on two-way ANOVA with post-hoc Tukey's test.*

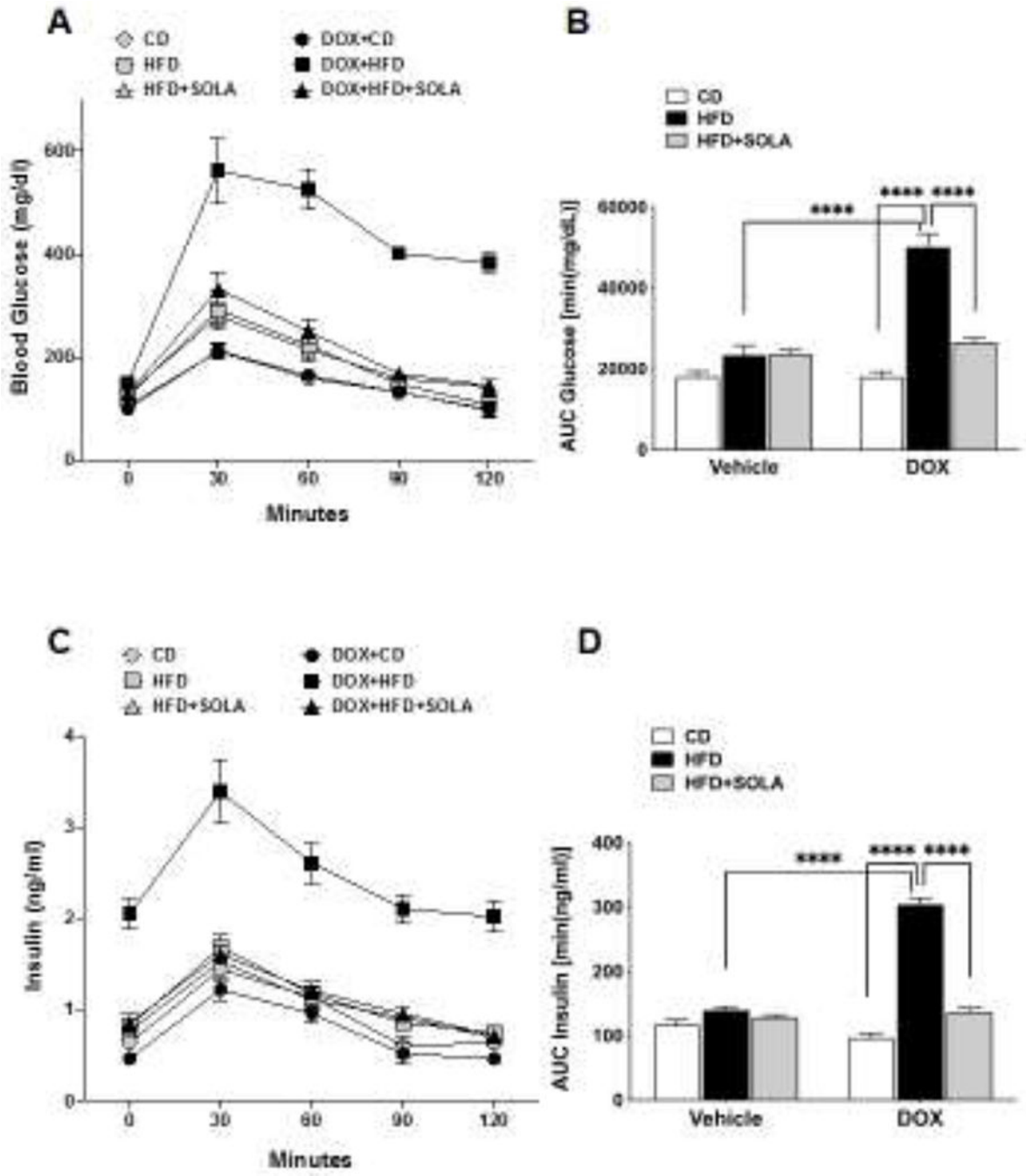

Figure 4:

(A) Blood glucose and (C) Plasma Insulin in over a time course of 2 hours after an intraperitoneal glucose challenge of 2 g/kg body weight. Area under the curve (AUC) for (B) plasma glucose and (D) plasma insulin calculated using standard trapezoid method (n=5-8 per group); CD, Control diet; HFD, High fat diet; DOX, Doxycycline; SOLA, 20-HETE antagonist; ****$p<0.0001$ *based on two-way ANOVA with post-hoc Tukey's test.*

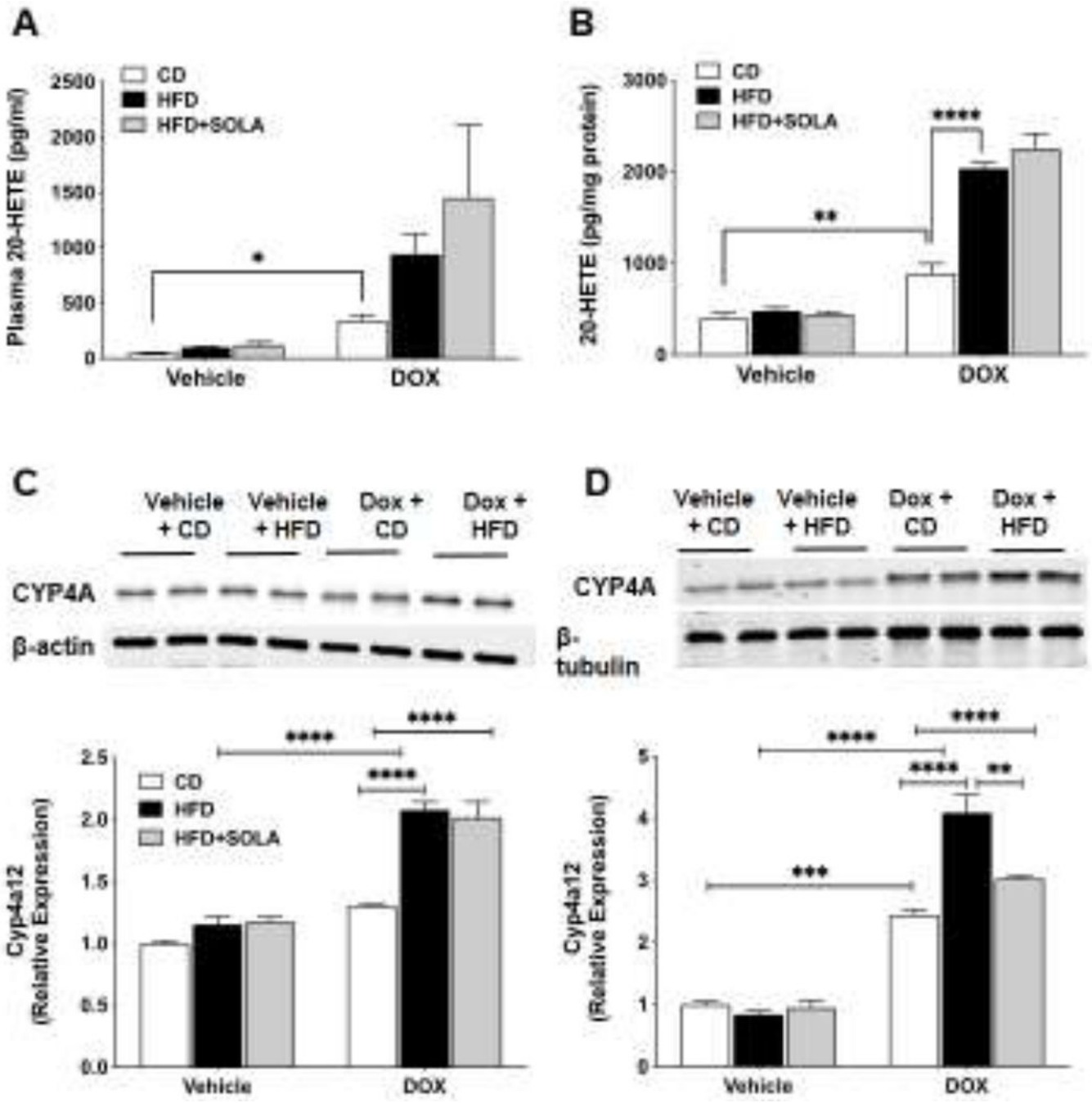

Figure 5:

20-HETE levels in (A) plasma and (B) adipose tissue of Cyp4a12tg mice post 15 weeks of diet feeding. Representative western blots and densitometry analysis of Cyp4a protein in (C) skeletal muscle and (D) adipose tissue. Quantitative protein expression is normalized to β-actin (for adipose tissue) and β-tubulin (for skeletal muscle). CD, Control diet; HFD, High fat diet; DOX, Doxycycline; SOLA, 20-HETE antagonist; n=4-5 per group; *$p<0.05$, **$p<0.01$, ****$p<0.0001$ *based on two-way ANOVA with post-hoc Tukey's test.*

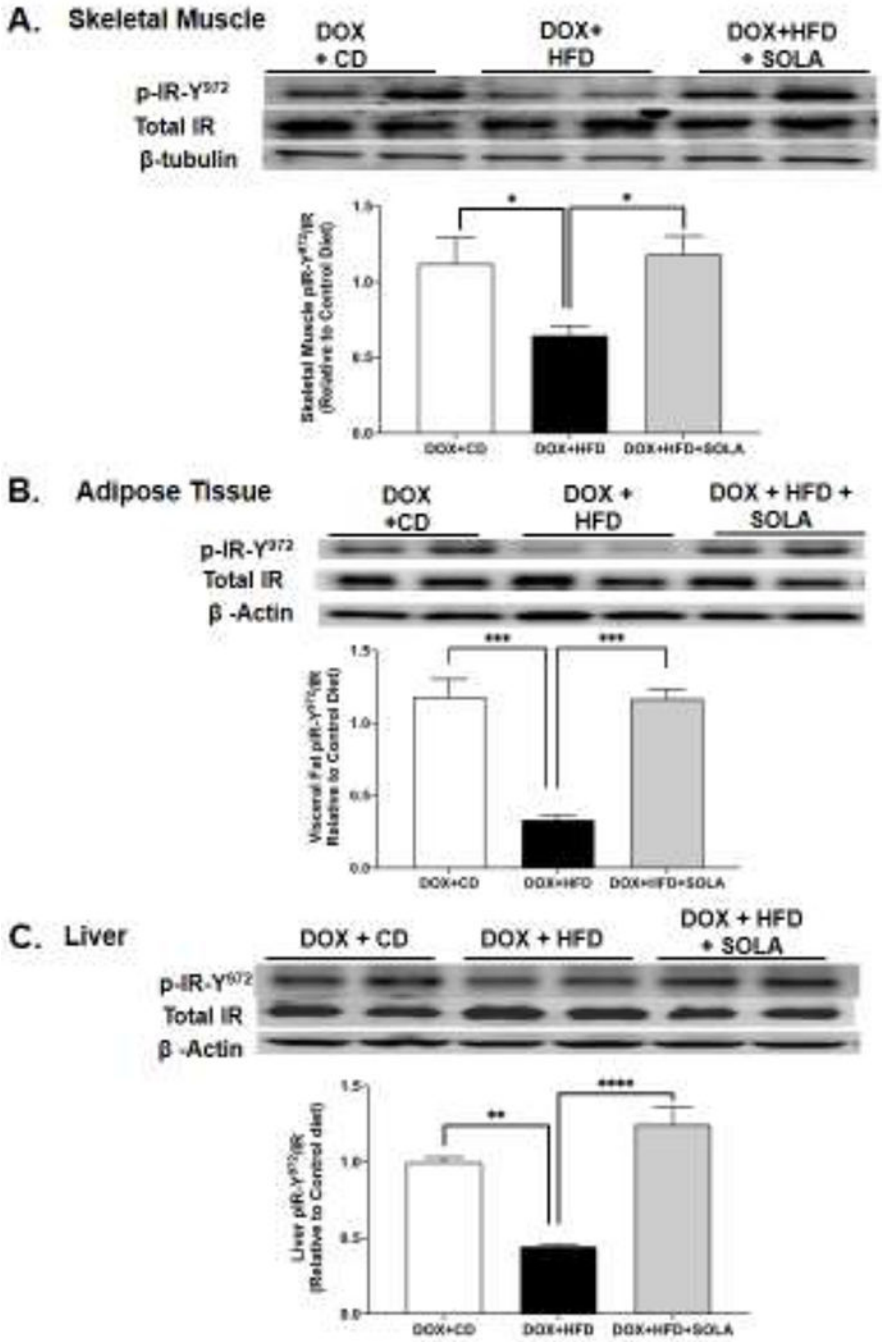

Figure 6:

Representative western blots and densitometry analysis of Tyr-972 phosphorylated insulin receptor in (A) skeletal muscle, (B) adipose tissue, and (C) liver of Cyp4a12tg mice post 15 week of diet feeding. Quantitative protein expression is normalized to total insulin receptor as a loading control (n=4-6 per group); CD, Control diet; HFD, High fat diet; DOX, Doxycycline; SOLA, 20-HETE antagonist; *$p<0.05$, **$p<0.01$, ***$p<0.001$, ****$p<0.0001$ *using one-way ANOVA with post-hoc Tukey's test.*

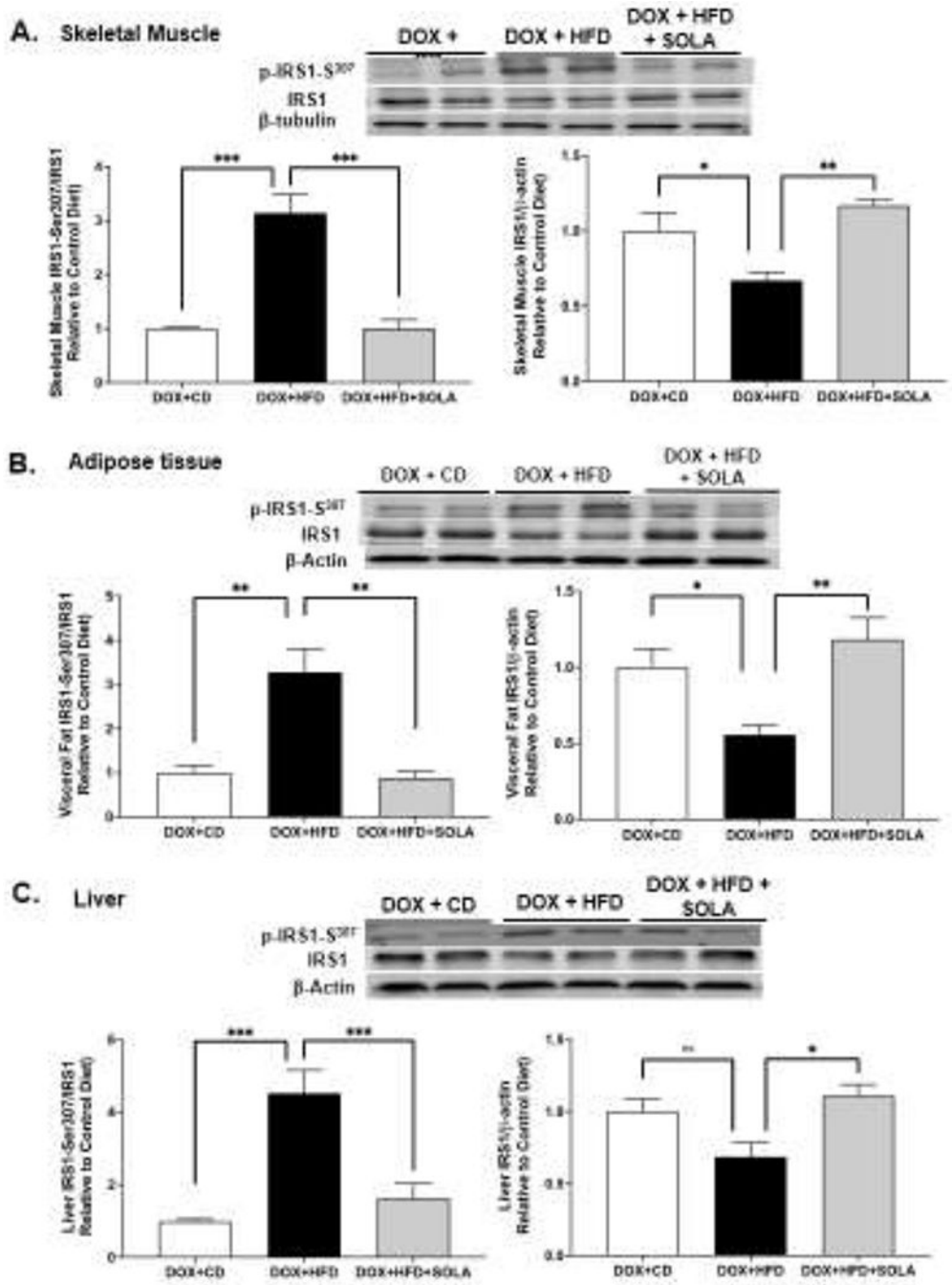

Figure 7:

Representative western blots and densitometry analysis of Ser-307 phosphorylated and total insulin receptor substrate-1 in (A) skeletal muscle, (B) adipose tissue and (C) liver of Cyp4a12tg mice. Quantitative protein expression is normalized to IRS-1 (for p-IRS1-ser307) and to β-actin/β-tubulin (for IRS1) as loading control (n=4-6 per group); CD, Control diet; HFD, High fat diet; DOX, Doxycycline; SOLA, 20-HETE antagonist; **p<0.05*, ***P<0.01*, ****p<0.001, using one-way ANOVA with post-hoc Tukey's test.*

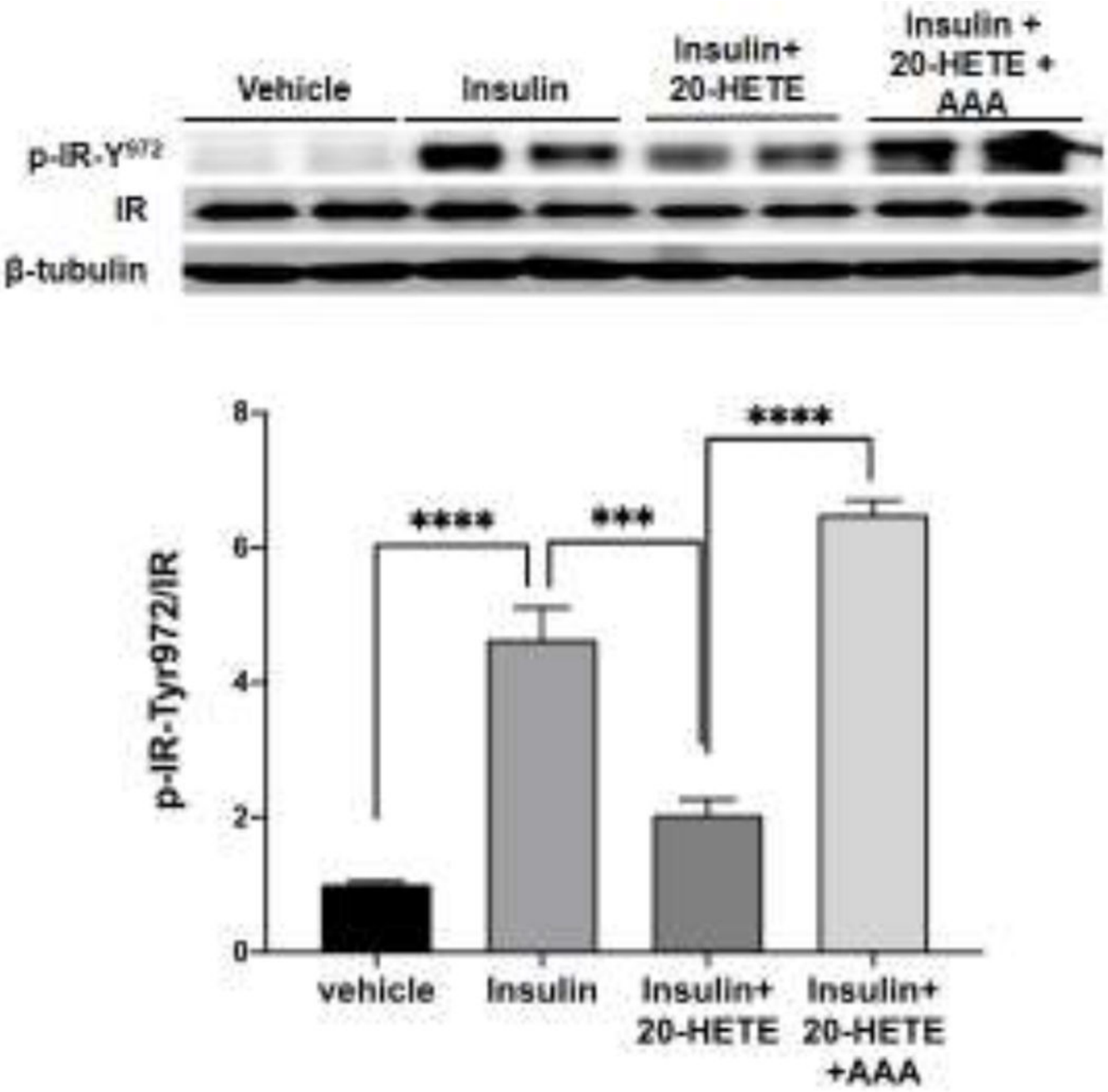

Figure 8:

Representative western blots and densitometry analysis of Tyr972 phosphorylated insulin receptor in differentiated 3T3L1 adipocytes stimulated with insulin following preincubation with i) vehicle, ii) 20-HETE and iii) AAA (20-HETE receptor antagonist) and 20-HETE. ****p<0.001, ****p<0.0001 using one-way ANOVA with post-hoc Tukey's test.*